Extended sources near-field processing of experimental aperture synthesis data and application of the Gerchberg method for enhancing radiometric three-dimensional millimetre-wave images in security screening portals

Neil A. Salmon
Manchester Metropolitan University, Manchester, M15 6BH, UK

ABSTRACT

Aperture synthesis for passive millimetre wave imaging provides a means to screen people for concealed threats in the extreme near-field configuration of a portal, a regime where the imager to subject distance is of the order of both the required depth-of-field and the field-of-view. Due to optical aberrations, focal plane array imagers cannot deliver the large depth-of-fields and field-of-views required in this regime. Active sensors on the other hand can deliver these but face challenges of illumination, speckle and multi-path issues when imaging canyon regions of the body. Fortunately an aperture synthesis passive millimetre wave imaging system can deliver large depth-of-fields and field-of-views, whilst having no speckle effects, as the radiometric emission from the human body is spatially incoherent. Furthermore, as in portal security screening scenarios the aperture synthesis imaging technique delivers a half-wavelength spatial resolution, it can effectively screen the whole of the human body.

Some recent measurements are presented that demonstrate the three-dimensional imaging capability of extended sources using a 22 GHz aperture synthesis system. A comparison is made between imagery generated via the analytic Fourier transform and a gridding fast Fourier transform method. The analytic Fourier transform enables aliasing in the imagery to be more clearly identified. Some initial results are also presented of how the Gerchberg technique, an image enhancement algorithm used in radio astronomy, is adapted for three-dimensional imaging in security screening. This technique is shown to be able to improve the quality of imagery, without adding extra receivers to the imager. The requirements of a walk through security screening system for use at entrances to airport departure lounges are discussed, concluding that these can be met by an aperture synthesis imager.

Keywords: Aperture synthesis, imaging, security screening, Gerchberg, aliasing, portal, three-dimensional, millimetre wave, terahertz, near-field

1. INTRODUCTION

The opportunity for the millimetre wave band to be used for security screening first came about through considerations in the 1970's about how this technology might be used to detect the unauthorised traffic of radioactive materials on persons from nuclear installations. In the 1980's large (several GHz) bandwidth GaAs amplifier and mixer technology enabled the feasibility of millimetre wave security screening for concealed weapons and illegal items under persons clothing to be explored more fully. By the end of the 1990's, the capabilities of radiometric (or passive) millimetre wave imaging for security screening had been explored comprehensively, identifying the band from 20 GHz to 300 GHz as potentially useful for portal to stand-off security screening of people. This capability was demonstrated in this period by the many high quality static and real-time imaging systems.

Around the year 2000 it became clear that the market demand for a portal screening system was for one that had a depth-of-field and field-of-view commensurate with the portal screening volume, which was something like two cubic metres. Delivering this in a passive imaging system using quasi-optical type components was extremely challenging, because in the near-field fundamental limits of optical aberrations (of lenses and mirrors) prevents achievement of adequate depth-of-field and field-of-view.

* Correspondence: Email: n.salmon at mmu.ac.uk; Telephone: +44 7921172892

About the same time synthetic aperture millimetre wave radar systems, which routinely operate in the near-field (albeit at kilometre ranges) delivering large depth-of-field and field-of-view, began to demonstrate powerful imaging capabilities for the portal screening market. A passive equivalent in the form of an aperture synthesis system can also deliver the large depths-of-field and wide field-of-views [1]. This is because no optical components are used. Furthermore it does this in the absence of speckle and multipath associated with the active (ie. coherently illuminating) systems, as it images only spatially incoherent emission from the person. An aperture synthesis portal system would take the form of an array of antennas linked to a digital cross-correlator [2]. In such a system for a full body walk-through three-dimensional screening portal, the subject would actually step inside an array is inwardly directed antennas. The speed of image acquisition is faster than the person can move; so many blur-free images of varying perspectives may be taken as the person transits the screening portal.

The content of this paper contains in part technical details about how this vision may be realised. Some experimental imagery is examined and the effects due to algorithms based on an analytic Fourier transform and the gridding fast Fourier transform (FFT) method of creating the image are compared. A technique referred to as the Gerchberg method is described and used to demonstrate how this can be used improve the quality of imagery. The requirements are described of a walk-through security screening portal for use at the entrances to airport departure lounges.

The work in this paper has been partially funded by the UK, Department for Transport, under the UK Government Future Aviation Security Solutions (FASS) programme.

2. THREE-DIMENSIONAL IMAGE GENERATION THEORY

The aperture synthesis imaging capability exploits the coherence properties of radiometrically generated radiation. Just how this can lead to an imaging capability is far from obvious, but the technique has been rigorously demonstrated by the radio astronomers for a number of decades by creating two-dimensional images of astrophysical sources. When applying this technique to the near-field it enables a three-dimensional imaging capability, providing the Abbe microscope, half-wavelength spatial resolution, as outlined in [1]. An ideal application of this is for a security screening portal for the aviation security industry.

The technique exploits the fact that the cross-correlation ($V'_{J,K}$) given by

$$V'_{J,K} = \left\langle v_J(t) v_K^*(t) \right\rangle \tag{1}$$

of the electric fields (v_J and v_K) at two locations in space, having position vectors $\mathbf{R}_J$ and $\mathbf{R}_K$, from the radiometric emission from an object, represents one Fourier component of the spatial frequencies of the image of that object. This means that if sufficient numbers of spatial frequencies can be collected, an inverse Fourier transform of these can be used to create the image. This Fourier transform relationship between the cross-correlations and the image is one in three-dimensions and it is referred to as the van Cittert Zernike theorem [3]. The discretised inverse transform of this, used to generate the three-dimensional image is given by

$$I(\mathbf{l}) = \left[A(\mathbf{l})\right]^{-1} \sum_{J,K,J\neq K}^{n(n-1)/2} V(\mathbf{u}_{J,K}) exp\left(i\mathbf{u}_{J,K}.\mathbf{l}\right), \tag{2}$$

where $\mathbf{l}$ is the direction cosine vector of the image voxel from the phase centre, $\mathbf{u}_{J,K}$ is the spatial frequency vector and $V_{J,K}$ ($\mathbf{u}_{J,K}$) is referred to as the visibility function and contains the phase-corrected cross-correlations defined by

$$V_{J,K}(\mathbf{u}_{J,K}) = V'_{J,K}\, exp\left(-i\phi_{J,K,CAL}\right). \tag{3}$$

This phase correction is effectively a phase calibration of the cross-correlations and results in centring the 3D image at a defined phase centre in space, having a position vector $\mathbf{R}_{PC}$. The phase calibration factor $\phi_{J,K,CAL}$ can be determined by measuring a noise source placed at the phase centre, or at an adjacent defined location. The spatial frequency in three dimensions, by definition [4], is represented by the vector

$$\mathbf{u}_{J,K} = \nabla\phi_{J,K}, \tag{4}$$

where $\phi_{J,K}$ is the phase of the cross-correlation (a scaler function) from a source at the phase centre of the image and ∇ is nabla, the spatial gradient operator. Vector calculus on the last equation indicates the spatial frequency vector abscissa in 3D space is given by

$$\mathbf{u}_{J,K} = \frac{2\pi}{\lambda}\left(\frac{\mathbf{R}_J - \mathbf{R}_{PC}}{|\mathbf{R}_J - \mathbf{R}_{PC}|} - \frac{\mathbf{R}_K - \mathbf{R}_{PC}}{|\mathbf{R}_K - \mathbf{R}_{PC}|} \right). \tag{5}$$

There are two possible routes to determining the image from the Fourier transform of Eq. 2. The first of these is the analytic Fourier transform, referred to by the radio astronomers as the direct Fourier transform [5], which is the transformation of in Eq.2. The benefit of this is that there is no intermediate processing of data that may lead to image artefacts, but the disadvantage is that computationally it can be quite intensive, particularly if there are many receivers and voxels in the image. This is compounded by the fact that for n receivers, there will be $n(n\text{-}1)/2$ complex cross-correlations. Given the complexity of Fourier transforms by this method rises as the square of the number of points, the complexity of the transform is proportional to n^4.

The second route is referred to as the Fourier transform gridding route. Here a regular grid in 3D visibility space is set out on to which the phase corrected cross-correlations, $V_{J,K}$ are interpolated. With the cross-correlations interpolated to the regular grid a discreet Fourier transform (DFT) can be used, which is then calculated using the Fast Fourier Transform (FFT). This has the advantage of being extremely quick for the computation, but it does introduce small errors arising from the interpolation on to the regular grid. Using the FFT the complexity of the transform reduces, from n^4 for the analytic transform, to ~ $n^3 log(n)$.

Using this method the resolution within the portal can be half wavelength, this means by operating at about 20 GHz the voxel size can be around 1 cm cube. With an imaging volume of 2 m^3 this means there are 2M voxels inside the portal. There may be hundreds of receivers in the array so efficient computation is needed.

3. EXPERIMENTAL IMAGES VIA THE ANALYTIC FT AND THE GRIDDING FFT

A series of images of a domestic iron covered with absorber generated by the analytic Fourier transform and a gridded FFT are shown in Figure 1. The absorber is 15.5 cm across by 24 cm high and approximately iron shaped, and it is located 40 cm from the imaging array. About 15 minutes after the iron has been switched on the temperature of the centre area of the absorber surface reaches a steady value of 57 °C. There is only one iron in the field of view but using the analytic FT route (left side of Figure 1) there appears one central image of the iron, surrounded by six others, with faint ghost of images in a regular pattern. The total of one-plus-six images of the iron illustrates the effects how the image repeats in real space, when created from samples in the Fourier space. However, the six surrounding images are outside the unit circle in direction cosine space, as can be seen in the lower part of the figure, so effectively is not part of the image and could be removed. They are shown just to illustrate the principle. In the terminology of phased array radar these artefacts are referred to as grating lobes.

The faint ghosts of the iron are real aliases in that they are located within the unit circle of the direction cosine. These are due to the imperfect sampling of the antenna array, which means there are some holes in the spatial frequency space and these occur towards the edges of the visibility function. These do not manifest themselves in the central region of the image, only around the periphery of the image. The faint ghosts could be dispersed, so they are almost unnoticeable, by fully filling the array with antennas of randomising the positions of a sparser array, so they are no longer on a regular grid. The effects of this dispersion are manifested as a small additive additional noise in the image.

It is noted in the image form using the analytic Fourier transform that in the region between the aliases the emission levels are fairly uniform. This is because this data is taken indoors with no ‘cold’ sky radiation entering through windows, which means the radiation temperatures of all surfaces are held at the thermodynamic temperature of the room, set by the central heating at typically ~22°C; the room is effectively a black body cavity at this temperature. Furthermore when the iron is move physically in space, aliases move with the central image, and the intensities between the aliases remain consistently low. The conclusion of this is that the only identifiable artefacts in the image are those due to aliasing, with essentially no other observed effects. Therefore, for improved imaging, aliasing has to be either removed, or the effects of it minimised.

In the case of the imagery created using the gridding FFT algorithm (right side of Figure 1), the effects of aliasing are

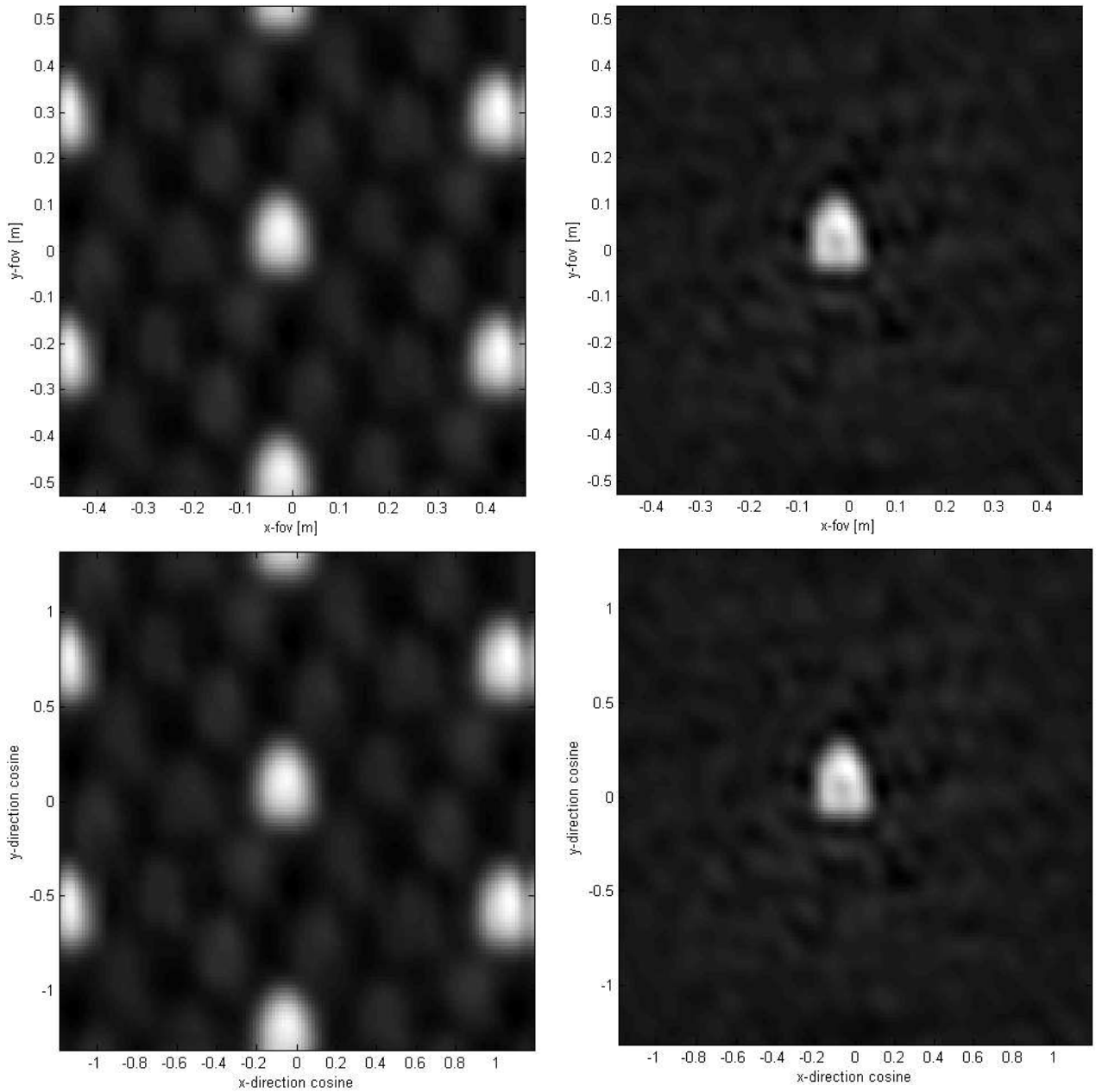

Figure 1: Images shown with axes in metres (upper) and direction cosines (lower) illustrating effects of the analytic Fourier transform (left) and the gridding fast Fourier transform (right) in the creation of the image from experimentally measured cross-correlations.

more difficult to identify. This is because they are masked by the effects of the interpolation of the measured visibilities (or cross-correlations) on to the spatial frequency regular spaced abscissa. It is noted that there is only one central image of the iron but that it is surrounded by a noise-like structure. It is also noted that when the iron physically moves the noise-like structure also moves but also changes in structure. The interpretation of this is that the interpolation is creating new samples of the visibility function, so in a sense is behaving as non-linear deconvolution, as new information is being added. This has the effect of removing the grating lobes and dispersing the effects of the alias which are visible in the analytic FT route. It is therefore highly likely that image artefacts in the gridding FFT route imagery are essentially those of aliasing, but it is more difficult to appreciate this fact, without evaluating the analytic FT imagery first.

Absolute calibration of the system is possible as the iron has a known thermodynamic temperature of 57°C. There is the assumption here that as the absorber is a radiating source, its radiation and thermodynamic temperatures are the same. This is used to calibrate the system absolutely and therefore this can be used to measure the radiation temperature of other sources in the field-of-view.

4. GERCHBERG-SAXON PAPOULIS METHOD

The Gerchberg-Saxon Papoulis method, first described in [6], is a technique for improving the quality of an image, by adding known information that comes from the object. The idea is that the Fourier space measurements (ie the cross-correlations) can be complemented with information about the objects to create a better image. The technique was first applied to improve the diffraction limited two-dimensional imagery from radio astronomy aperture synthesis systems. The known information is that some regions of the image can be assumed to have zero intensity and that all other regions must have an intensity equal to or greater than zero. Use of the algorithm for two-dimensional aperture synthesis imaging for radio astronomy, is described in [7]. The work here adapts the technique for use in three-dimensional aperture synthesis imaging in a security screening portal.

The technique exploits additional information about the object to improve the image quality from that due to the millimetre wave aperture synthesis 3D imaging algorithms alone. Valuable information such as the position of the object can be perhaps measured by 3D optical imager or a positional scanner. It is known from the physics of millimetre wave interaction with the human body that because the body is so attenuating, no radiation travels further than a fraction of a millimetre. It is also known from the physics of millimetre wave interaction with the atmosphere that no radiation is generated from the empty air space surrounding an object, in a prospective security screening portal. It is therefore a reasonable assumption that millimetre wave radiation measured from within a portal only originates from a thin shell in 3D space comprising: the clothing of a person, any possible threat items and a fraction of a millimetre depth into the human skin [10]. This is valuable information when creating a 3D millimetre wave image of a person in a security screening portal.

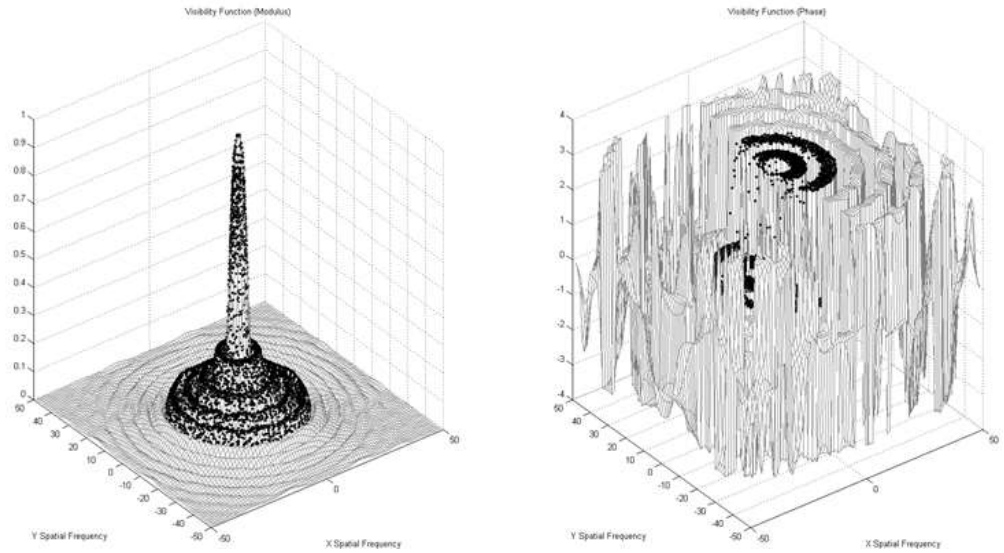

Figure: 2 A slice through the 3D visibility function showing the magnitude (left) and phase (right) as a rectangular mesh grid together with the sampled visibilities from the antenna array after 20 iterations of the Gerchberg method using simulated cross-correlations from a spherical shell of radiators, with the image from this shown in the left side of Figure 3.

The aperture synthesis technique enables a 3D image to be generated. However, to satisfy requirements on aliasing many receivers need to be used to create sufficient numbers of samples of the 3D visibility function in Fourier space. The

Gerchberg method enables deficits in samples of the visibility function to be compensated for, by providing information about the object (from real space). It is an iterative technique whereby the measured (or simulated) visibilities in Fourier space are used together with known information about the image in real space. The known information in real space is that the intensity outside and inside the radiating shell is zero. The unknown information is that the intensity of the shell itself must be between zero and some positive value. By adding the known information in real space then transforming this to Fourier space and adding the measured cross-correlations, then back to real space enables successively more accurate estimates to be determined of the unknowns of the emission associated with the shell. This shell structure then constitutes the image in 3D space and can be viewed from any orientation using 3D computer graphics or analysed by machine to identify anomalies.

The Gerchberg method as outlined above has been trialled by simulation of the imaging of a 20 cm diameter radiating sphere located at the centre of an array of 359 inwardly pointing antennas located on a surface of a 2 m diameter sphere. The simulation was performed at 3.71 GHz ($\lambda \sim 8$ cm) as better convergence was found at these frequencies than at higher ones. The visibilities in the simulation were calculated using the method outlined in [1]. The zeros of intensities were set in the image in those regions further than $(0.7)\lambda/2$ from the centre of the radiating shell. Visibilities at spatial frequency locations closer than half the minimum antenna separation from any known visibility value assumed a value from a (3D) interpolation from the known visibilities. Those visibilities at spatial frequencies further than half the minimum antenna spacing were allowed to have their values determined by the iterative process.

The results of applying the Gerchberg method are shown on the visibility function and image in Figure 2 and 3 respectively after a series of 20 iterations. Both the visibility function and the image are 3D functions, so only x-y slices through the centre of these functions are shown. The slices through the x-y, x-z and y-z planes are essentially the same, so only slices through the x-y plane are shown. In the case of the visibility function, as this is complex, phase and magnitude are shown. The visibility function as generated by the Gerchberg method is displayed as a mesh grid, whilst the samples of visibility created from the antenna locations and the coherence function from the objects are displayed as crosses. The visibility mesh extends to higher spatial frequencies than those measured because the act of confining the image through the zeros of intensities brings in higher spatial frequencies than those measured directly by the receivers.

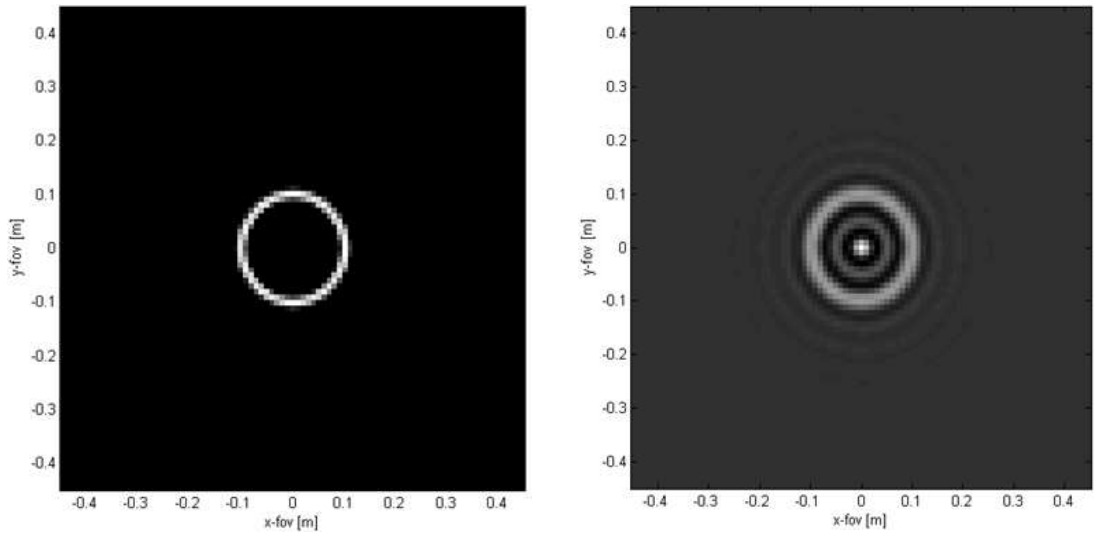

Figure 3: Images showing the effects of the Gerchberg method on the three-dimensional image of a spherical radiating surface, using the FFT gridding method in a simulation. The images show a two-dimensional slice of the three-dimensional image obtained using the 3-D aperture synthesis imaging technique, after 20 iterations of the Gerchberg method (left) and without the use of the method (right).

The 2D image as a slice through the centre of the 3D image from the Gerchberg method in Figure 3 indicates how the emission is localised to a ring. This corresponds to the emission from the surface as a slice through the centre of the radiating sphere. The figure shows the effects of the 3D aperture synthesis imaging algorithm, with and without the Gerchberg method. It can be seen that without the Gerchberg method there is ringing in the intensities around the ring, bearing in mind the wavelength is only 8 cm and the diameter of the sphere is only 20 cm. The microscope resolution at

half wavelength is only 4 cm at this radiation frequency. The Gerchberg method in confining the emission to within the resolution limit then introduces the higher spatial frequencies, as can be seen in Figure 2.

To monitor the convergence process two errors are plotted, these are firstly the RMS deviation in the phase between the known values of visibility and those determined by the Gerchberg method, and the RMS deviation in the fractional magnitude of the visibility between the visibilities determined by the Gerchberg method and the measured visibilities. These errors are shown for a series of 20 iterations in Figure 4.

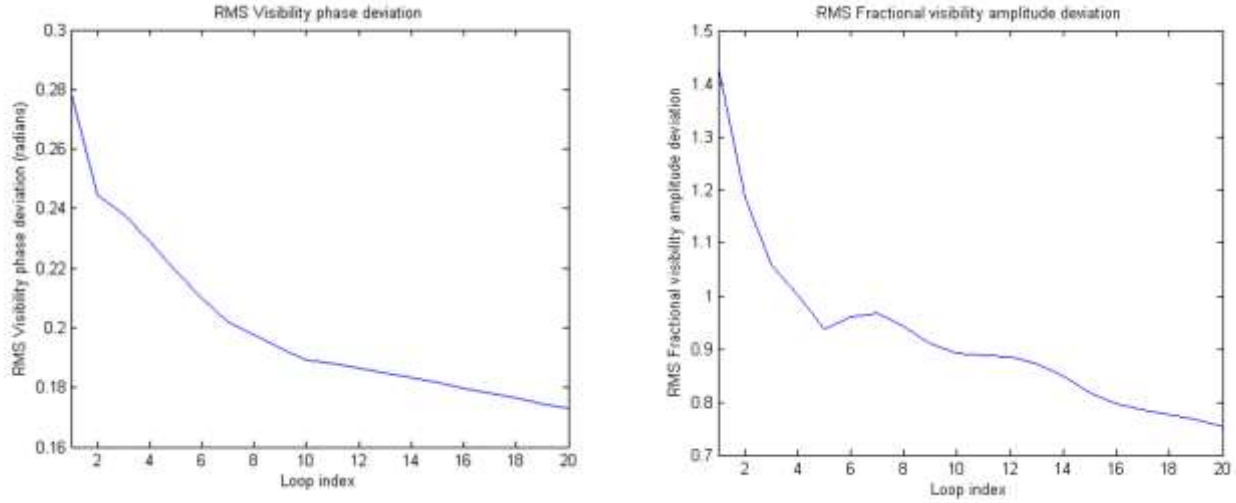

Figure 4: The RMS deviation of the visibility phase error (left) and the RMS fractional visibility amplitude error (right) determine by the Gerchberg method as a function of loop index, up to a maximum of 20 iterations. Convergence beyond 20 iterations is slower.

5. REQUIREMENTS FOR WALK-THROUGH PERSONNEL SECURITY SCREENING

A recent feasibility study examined the requirements of a security screening portal to screen people for items concealed on (but not inside) a person when they enter an airport departure lounge. From the airport operator perspective these screening systems need to be real-time and introduce no delays to passengers. This means the systems need to screen the full body of a person and evaluate the data for potential threats in the time it takes a person to walk a few metres. This requirement for speed is dictated by the market; passengers don't want to be standing in queues and airport operators want passengers to spend more time in the pleasant surroundings of the departure lounge.

For this screening process to be effective every surface of the human body needs to be accessible to the portal screening system. In a walk-through system this may be an advantage, as concealment of items on a person is more difficult if they are being forced to walk while being screened, than it is if a single static image is taken. For every surface region of the body to be view the passenger must walk through an archway of receiving antennas. To get a perspective of all bodily surfaces a passenger would be required to transit the portal with arms raised, so a good view of underarms, armpits and the side of the body is revealed. As views tangential to the human body reveal little information (as reflectivity rises to unity and emissivity falls to zero) antennas need to view all bodily surfaces as close to normal incidence as possible. Reception of circularly polarised radiation is beneficial in this respect as reflectivity of the human body remains constant as a function of angle of incidence out to about 85°, meaning contrast of threats against the body remains high over larger areas of the image, therefore giving more chance for them to be recognised. This has the effect of maximising probability of detection and minimising false alarms. This is most conveniently approximated by having receivers on the floor and above the subject, so the screening portal takes on the form of a short corridor possibly 20 cm to 40 cm long, approximately 1 metre across, by ~2 metres high.

It is well-known in the industry that persons intent on concealing items on their person place these in regions of the body which are difficult to screen well in a pat-down search or with existing active millimetre wave screening portals. These regions are: between the legs, groin, intergluteal cleft, arm pit, folds of flesh, breast cleavage, directly below the breasts, tops of shoulders; the head (items concealed in wigs and other types of headwear) and around the waist belt. These

regions of the human body are generally those where there is curvature of the surface, complex three-dimensional structure and canyons or crevice regions. A passive millimetre wave imaging system is ideal for imaging these regions of the body, as there are no speckle or multipath problems. An imaging system that introduces no artefacts due to the imaging process itself, only delivering a faultless image of the subject, is one that will deliver the low false alarm rate demanded by the aviation security industry.

A general consensus of opinion amongst those working in millimetre wave imaging is that a spatial resolution of about one-centimetre is sufficient to detect threats of interest for aviation security. Measurement and fundamental theory indicates an aperture synthesis portal screening system should be capable of a spatial resolution of between λ and $\lambda/2$. A system operating in the region of 20 GHz would therefore deliver the required centimetre spatial resolution. The system should also have a radiometric sensitivity in the region of 100 mK, as this will enable detection of a wide variety of non-metallic threats under clothing against the human body. This level of sensitivity will require an aperture synthesis system with hundreds of antennas/receiving channels and radiation bandwidth of the order of 1 GHz. This combined capability of spatial resolution and sensitivity will enable the high probability of detection demanded by the aviation security industry.

Machine anomaly (ie. potential threat) detection is required to be used with any portal screening system. This is what the end user community is saying about the airport screening scenario and it arises from the short amount of time allocated to screen each passenger and not because of privacy issues. Given that a PMMW imaging system would be delivering a spatial resolution of around 1 cm it is very unlikely that an operator would be able to effectively screen a person in a few seconds, given the complex human body geometry which has on average and area of ~19,000 cm^2 for a typical male. However, this is an ideal task for a machine, provided the input data is of sufficient quality.

Machine anomaly detection requires an accurate model of the skin of the human body. Accurate data about how the signature of human skin looks is only just emerging. The levels of emission (and reflectance) are shown to be varying consistently over the different regions of the body, with age, gender and ethnicity [9],[10]. Exploiting this kind of machine based analysis will make for a screening system which is impossible to deceive.

6. CONCLUSIONS

The theory enabling 3D imaging of sources is presented. This is used on experimental data to demonstrate that the technique can be used to image the extended source of a domestic iron covered with millimetre wave absorber in the near-field, 40 cm from the antenna array of the aperture synthesis imager. With a person as the subject, this scenario is not too dissimilar to a walk-through security screening portal.

The effects of two algorithms, based on the analytic Fourier transform and the gridding FFT methods, used to create images from experimentally measured data are compared. From this it is concluded that the only detrimental features in the resulting images arise from aliasing. Aliasing as the origin of these artefacts is much more apparent in the analytic Fourier transform images than those created using the gridding FFT method. This indicates future demonstrators should seek routes to minimising the effects aliasing, by for example selecting particular geometries of randomised antennas.

The Gerchberg method as 2-D image enhancement technique from radio astronomy has been adapted for 3-D imaging in the near field, demonstrating, by simulation, improved imagery. The method has been shown to be effective in delivering better resolved imagery and in creating additional spatial frequency information, some of this at higher spatial frequencies than measured by the antenna array.

The requirements are given for a whole body walk-through security screening portal for use at the entrances to airport departure lounges. An important part of these requirements is that all regions of the body must be screened effectively with centimetre spatial resolution, including cleavage regions, between the legs and under arms. High quality images of passengers moving through such a portal screening system could only be effectively assessed for threats and anomalies in the time available by a machine. Machines are ideally suited to these types of tasks.

7. FUTURE WORK

The aperture synthesis technique could be used to develop an effective full body screening system for use at entrances to airport departure lounges. The concept would be a short corridor covered on all sides, including top and bottom, with aperture synthesis antennas. The next milestone to this goal would be to develop one part of this, a system that would

generate in the region of 2000 pixels, to demonstrate quality imagery of tenuous non-metallic threats concealed in those regions of the body that are currently difficult to screen, namely cleavage and canyon areas. Refinement of the Gerchberg technique is required to establish optimum numbers of antennas for 3-D imaging walk-through portal systems.

REFERENCES

[1] Salmon, N. A.,"3-D Radiometric Aperture Synthesis Imaging", IEEE TMTT, Vol. 63, Issue 11, (2015).

[2] Salmon, N. A. Wilkinson, P.N. and Taylor, C., "Interferometric aperture synthesis for next generation passive millimetre wave imagers", SPIE Europe Security+Defence Europe, 'Millimetre Wave and Terahertz Sensors and Technology V', Edinburgh, September, (2012).

[3] Born, M., and Wolf, E., "Principles of optics", Cambridge University Press, 7th Edition, (2003).

[4] Goodman, "Introduction to Fourier Optics", 3rd Ed., Roberts & Company, (2005).

[5] Thomson, A., Moran, M., Swenson, G, "Interferometry and Synthesis in Radio Astronomy", Wiley, (2004)

[6] Gerchberg, R. W. "Super-resolution through Error Energy Reduction", Optica Acta: International Journal of Optics, vol. 21, no. 9, pp. 709-720, (1974), DOI: 10.1080/713818946.

[7] Starck, J-L and Murtagh, F., in Chapter 3, 'Deconvolution' of "Astronomical Image and Data Analysis", 2nd Ed. Springer, (2006).

[8] Salmon, N. A. "Simulations of three-dimensional radiometric imaging of extended sources in a security screening portal", SPIE Europe Security+Defence Europe, 'Millimetre Wave and Terahertz Sensors and Technology VIII, Toulouse, September, (2015).

[9] Owda, A., Rezgui, N-D, Salmon, N.A., "Signatures of human skin in the millimetre wave band (80-100) GHz", this conference

[10] Owda, A. Salmon, N.A., Harmer, S., Shylo, S., Borwing, N.J., Rezgui, N-D, Shah, M., "Millimeter-Wave Emissivity as a Metric for the Non-Contact Diagnosis of Human Skin Conditions" Journal of Bioelectromagnetics, vol. 38, issue 7, pp.559-569, DOI: 10.1002/bem.22074, October, (2017).